ACS EARTH AND SPACE CHEMISTRY

http://pubs.acs.org/journal/aesccq

Article

# Complexation by Particulate Organic Matter Alters Iron Redox Behavior

Prachi Joshi,* Laurel K. ThomasArrigo, Dennis Sawwa, Lea Sauter, and Andreas Kappler

Cite This: https://doi.org/10.1021/acsearthspacechem.3c00288

Read Online

ACCESS | Metrics & More | Article Recommendations | Supporting Information

**ABSTRACT:** The role of iron (Fe) in environmental redox processes, such as microbial respiration and pollutant turnover, is influenced by its association with organic matter, particularly in redox-dynamic systems such as wetlands. While the association between Fe and dissolved organic matter (DOM) has been studied extensively, the association between Fe and particulate organic matter (POM), which differs in size and composition from DOM, is poorly understood. In this work, we investigated the complexation of aqueous Fe(II) by mineral-free POM over a full redox cycle using wet chemical and spectroscopic (X-ray absorption and Mössbauer spectroscopy) techniques. The mass of Fe(II) complexed by POM under anoxic conditions ranged from 18.9 ± 1.2 mg Fe·g$^{-1}$ POM at pH 4.5 to 37.6 ± 1.5 mg Fe·g$^{-1}$ POM at pH 7. Part of the complexed Fe(II) was oxidized to Fe(III) (21−46%) under anoxic conditions, indicating that complexation by POM altered the Fe(II) redox stability. We then exposed POM-complexed Fe to $O_2$ at pH 5.5 and 7 to simulate oxidizing conditions. Upon exposure to aqueous $O_2$, the complexed Fe(II) was rapidly and completely oxidized at pH 5.5 and pH 7, faster than uncomplexed Fe(II), suggesting that complexation by POM promoted abiotic Fe(II) oxidation. The resulting Fe(III)-POM consisted of Fe(III)-organic phases and poorly crystalline Fe(III) (oxyhydr)oxides. The results of this work demonstrate that POM acts as a major complexant of Fe and alters Fe redox behavior, thereby affecting the role of Fe in environmental redox processes.

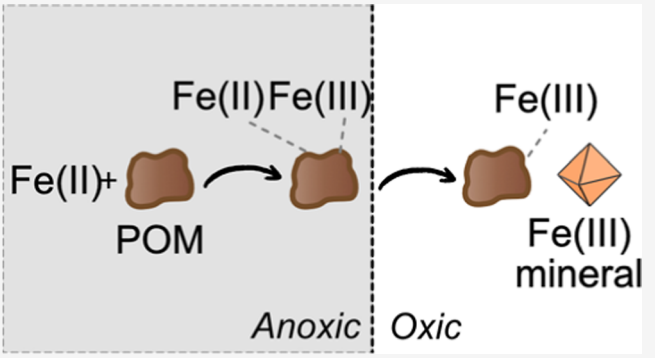


**KEYWORDS:** *organic matter, iron, redox cycling, metal complexation, X-ray absorption spectroscopy, Mössbauer spectroscopy*



## 1. INTRODUCTION

Iron (Fe) plays a critical role in environmental redox processes: it acts as a widespread electron acceptor (as ferric iron, Fe(III)) and an electron donor (as ferrous iron, Fe(II)) for microorganisms, thereby affecting the cycling of other elements such as carbon and phosphorus.[1−3] Ferrous iron (Fe(II)), often in combination with Fe(III) minerals, is also linked to the turnover of organic (e.g., TNT and nitrobenzene)[4−6] and inorganic pollutants (e.g., mercury and arsenic).[7−9] The redox reactivity of Fe is controlled by its association with other chemical species, namely, organic matter (dissolved organic matter, DOM, and particulate organic matter, POM). Association between Fe and organic matter may be in the form of complexation,[10−12] adsorption, and/or coprecipitation.[13−18] Such association has been observed in a wide variety of aquatic,[10,12,19] soil,[15−17] and sedimentary environments.[14,20] To predict the redox reactivity of Fe in these environments, it is therefore critical to consider the effect of organic matter association.

Past work has shown that the reduction potential of the Fe(II)/Fe(III) redox couple is altered by complexation with organic ligands,[11,21] affecting its role in abiotic[22] and microbial redox processes.[23] For example, complexation of Fe(II) with DOM analogues such as humic acid[21,24,25] and small organic molecules such as tannic acid[26] has been shown to inhibit oxidation of Fe(II) by oxygen, especially at low organic carbon/iron ratios. The presence of DOM has thus been invoked as the reason for the persistence of Fe(II) under oxic conditions, increasing its bioavailability.[19,23,27] In contrast, the promotion of Fe(II) oxidation due to complexation by DOM has been reported at high organic carbon/iron ratios,[28−30] for certain ligands (e.g., citrate),[26] or at low dissolved $O_2$ concentrations.[31] The effect of organic compound complexation on abiotic Fe(II) oxidation is therefore dependent on the environmental conditions as well as the identity of the complexing ligand. Further, the products of Fe(II) oxidation are affected by the presence of organic matter; recent evidence suggests that the presence of DOM and soil OM decreases the crystallinity of the resulting Fe(III) (oxyhydr)oxides.[25,32]

Received: October 10, 2023
Revised: December 28, 2023
Accepted: December 28, 2023

These poorly crystalline phases may be more bioavailable for Fe(III)-reducing microorganisms, promoting Fe turnover rates (shown recently in soil slurry experiments[33]). The altered redox reactivity of Fe(II) and Fe(III) due to association with organic matter is particularly important in environments that undergo redox fluctuations, e.g., wetlands. In such environments, aqueous Fe(II), formed as a result of dissimilatory Fe(III) mineral reduction, may be complexed by organic matter and later oxidized to a mix of (reactive) Fe(II)/Fe(III) phases, e.g., after water table drawdown. During subsequent anoxic periods, these Fe-organic matter phases may further associate with aqueous Fe(II) via the complexation of Fe(II) by organic matter and/or sorption of Fe(II) to any formed Fe(III) (oxyhydr)oxides. Thus, complexation by organic matter likely affects the behavior of Fe in redox-dynamic environments, with cascading effects on elemental cycling and pollutant turnover.

The majority of knowledge about the effect of organic matter complexation on Fe reactivity is based on studies focusing on soluble organic compounds (ligands, standard DOM compounds, or DOM analogues). In contrast, little is known about the association between Fe and larger size fractions of organic matter, i.e., POM, which may be more important relative to DOM in organic-rich systems such as wetlands.[34,35] DOM is generally defined operationally as the organic matter that passes through a 0.45 or 0.22 $\mu$m filter.[34,36] This fraction contains a mix of low-molecular weight compounds (e.g., proteins and carbohydrates) that are the product of enzymatic depolymerization or microbial processing.[34,37] Organic matter that is retained on the filter is defined as POM, which is dominated by plant-derived compounds (e.g., lignin and cellulose) with a small contribution of living and dead microbial biomass.[37,38] Therefore, the chemical compositions of these size fractions are different, likely resulting in different reactivities toward Fe.

Indirect evidence for the effect of complexation by POM of Fe redox behavior is given by past field studies in organic-rich soils.[12,39−41] Using spectroscopic techniques, Bhattacharyya et al. and Patzner et al. observed the presence of Fe(II)-organic matter and Fe(III)-organic matter phases under both oxic and anoxic conditions in peatlands in New York, USA[40] and Abisko, Sweden,[41] respectively. Evidence for Fe(II) complexation by POM has also been given by Chen and Thompson, who observed that the removal of organic matter from soils resulted in decreased aqueous Fe(II) uptake by the soil.[32,42] Although these studies suggest that POM complexes Fe and affects Fe redox stability, the general applicability of these results is limited by the effect of several environmental variables (e.g., underlying geology and precipitation patterns), motivating the need for a systematic study of Fe complexation by POM.

The overarching goal of this study was to investigate the complexation of Fe by POM under consecutive reducing and oxidizing conditions. Specifically, the objectives were to (i) determine the quantity of Fe that may be complexed by POM under anoxic conditions over time (pH 7) and as a function of pH (pH 4.5, 5.5, and 7), (ii) study the oxidation of POM-complexed Fe(II) upon subsequent exposure to oxic conditions (pH 5.5 and 7), and (iii) test the effect of exposing oxidized Fe-POM to aqueous Fe(II) under anoxic conditions at pH 7, thus simulating a complete redox cycle. Over the course of these redox changes, we followed the speciation of Fe using a combination of wet chemistry, X-ray absorption spectroscopy (XAS), and Mössbauer spectroscopy. We tested complexation under anoxic conditions at pH values of 4.5, 5.5, and 7 to represent the general range in wetland conditions (acidic to neutral), while we focused on pH 7 conditions for the subsequent oxidation and exposure of oxidized Fe-POM to aqueous Fe(II).

## 2. MATERIALS AND METHODS

**2.1. Chemicals.** All solutions were prepared with double deionized water (Barnstead MQ system, Thermo Fisher Scientific, Germany, >18 MΩ·cm). We used acetic acid ($pK_a$ = 4.75; Honeywell Fluka, Austria), MES [2-(*N*-morpholino)-ethanesulfonic acid, $pK_a$ = 6.15; Carl Roth GmbH, Germany, >99%], and MOPS [3-(*N*-morpholino)-propanesulfonic acid, $pK_a$ = 7.20; Carl Roth GmbH, Germany, >99%] as pH 4.5, 5.5, and 7 buffers, respectively. Acidic solutions were prepared from HCl (hydrochloric acid, Sigma-Aldrich, Austria, 37%). Ferrous chloride ($FeCl_2{\cdot}4H_2O$, Sigma-Aldrich, Germany, 98%) was purchased in a sealed container with $N_2$ headspace and opened directly inside the glovebox.

**2.2. Anoxic Working Conditions.** Complexation experiments and part of the oxidation experiments were conducted inside an anoxic glovebox (MBraun Unilab Workstation, 100% $N_2$ atmosphere, <10 ppm $O_2$). Aqueous solutions were purged with $N_2$ (Westfalen, Germany, 99.999%) for 2 h before being taken inside the glovebox. All glassware, plasticware, powdered chemicals, and POM were placed under vacuum overnight, taken into the glovebox, and remained inside the glovebox for 24 h prior to the start of the experiments. The aqueous Fe(II) stock solution was prepared from $FeCl_2{\cdot}4H_2O$ and stored inside the glovebox.

**2.3. Peat POM.** We used bulk peat "Floratorf" (Floragard, Germany), originating from ombrotrophic bogs, as POM. The POM had a high carbon content (45.6%, Vario EL III elemental analyzer) and negligible Fe (<0.1%) and Mn (<0.002%) contents (measured with ICP−MS after microwave-assisted digestion, details in Supporting Information, Section S1). These elemental contents are consistent with the carbon and metal contents of peat from ombrotrophic bogs.[38,43−45] For our experiments, we prepared the POM by first drying it at 30 °C for 24 h. The dried POM was then sieved (2 mm) to remove any large plant parts and milled (Retsch MM 400; 5 min at 990 rpm). We chose to mill the POM in order to (i) obtain a homogeneous batch of POM for all the experiments and (ii) enable recovery of the Fe-POM for later oxidation experiments as well as for spectroscopic analyses. Initial tests showed that without prior milling of the POM, all of the POM could not be reproducibly recovered after filtration, limiting our ability to collect the POM after complexation for later experiments. We note that milling may increase the accessible surface area of the POM. Fourier-transform infrared (FTIR) spectra of the peat POM indicate the presence of carboxylic, aromatic (including phenolic), and polysaccharide groups (Figure S1), similar to past studies of peat from ombrotrophic bogs.[46−48]

**2.4. Complexation of Fe(II) by POM.** We tested the complexation of Fe(II) (1 mM) by POM (1 g/L) in batch reactors at three pH values: 4.5 (25 mM acetate), 5.5 (25 mM MES), and 7 (25 mM MOPS). First, we determined the time scale of complexation between the POM and aqueous Fe(II) by setting up sacrificial batch reactors in which aqueous Fe(II) was exposed to the POM at pH 7 over 27 h under anoxic conditions. Reactors (20 mL serum bottles) were set up by


https://doi.org/10.1021/acsearthspacechem.3c00288
ACS Earth Space Chem. XXXX, XXX, XXX−XXX

adding a predetermined volume of buffer to the POM inside the glovebox (1 g/L POM). The reactors were sealed with butyl rubber stoppers, crimp-sealed, and mixed on a rolling shaker (60 rpm) for 1 h to hydrate the POM. A small volume of Fe(II) solution was then added to the reactors inside the glovebox in order to reach an initial aqueous Fe(II) concentration of 1 mM. The reactors were crimp-sealed again and placed on a rolling shaker (60 rpm). At several time points (15 min, 165 min, 5.5 h, 23 h, and 27 h), triplicate batch reactors were sacrificially sampled by opening the reactors inside the glovebox, withdrawing an aliquot (≈0.4 mL) of the reactor suspension, and filtering it using a syringe filter (0.45 μm, Fisher Scientific, Germany, PTFE). The concentration of aqueous Fe(II) and Fe(III) in the filtrate was measured spectrophotometrically using the ferrozine assay.[49] The complexation experiments at pH 4.5 and 5.5 were conducted similarly to the pH 7 experiment, except that the reactors were sacrificially sampled after 24 h based on the results of the pH 7 kinetic experiment. For spectroscopic analyses (detailed below), additional batch experiments were set up similarly. The solid phase was collected after 24 h using a syringe filter (0.45 μm, Fisher Scientific, Germany, PTFE), resuspended in the respective pH buffer (25 mM) that contained no Fe, and then freeze-dried anoxically. The freeze-dried solids from triplicate reactors were combined before homogenization inside the glovebox for spectroscopic analyses.

Two sets of control reactors were set up. For each pH, we set up duplicate POM-free reactors in order to determine the aqueous Fe(II) concentration. Further, to quantify the possible contributions of DOM released from the POM to the absorbance measured during the spectrophotometric determination of Fe, we set up triplicate Fe(II)-free reactors containing only pH buffer and POM (1 g/L). In all complexation experiments, the absorbance of the filtrate from these Fe(II)-free reactors, i.e., from DOM possibly leached from POM, was indistinguishable from the background absorbance.

**2.5. Oxidation of Fe-POM.** To investigate the oxidation of Fe(II) complexed by POM, we exposed the solids from the complexation experiments (hereafter referred to as "Fe-POM") to oxic conditions at pH 7 and pH 5.5 for 24 h. We first prepared Fe-POM by exposing POM (1 g/L) to aqueous Fe(II) (1 mM) for 24 h as in the complexation experiments above at pH 7. The Fe-POM was separated from the solution in each reactor using syringe filters (0.22 μm, Millipore, Germany, GTBP) inside the glovebox. An aliquot of the filtrate was used to measure the aqueous Fe(II) concentration. The filter with the solids was then placed in a new serum vial inside the glovebox and sealed. All of the serum vials were then taken out of the glovebox and opened, and oxic buffer (pH 7 MOPS, 25 mM) was added. The oxic buffer contained dissolved $O_2$ in excess (3×) of the $O_2$ required to oxidize the Fe(II) in the Fe-POM. The reaction vials were then closed with butyl rubber stoppers, crimp-sealed, and placed on a rolling shaker (60 rpm). Trial experiments showed that all the Fe-POM on the filter was resuspended in this step, and no Fe (Fe(II) or Fe(III)) or POM was left on the filter. At specific time points (5 min, 20 min, 2 h, and 20.5 h) after addition of the $O_2$-containing buffer, triplicate reactors were sacrificially sampled. First, two aliquots (1 and 0.3 mL) of the suspension were taken. The 0.3 mL aliquot was filtered (0.45 μm, Fisher Scientific, Germany, PTFE) and acidified with 1 M HCl to quantify the aqueous Fe(II) and Fe(III). The 1 mL aliquot was acidified (1 mL of 1 M HCl) to dissolve any Fe on the solids within the suspension. After 24 h, the Fe(II) and Fe(III) concentrations in the acid digest were measured. At each time point, the rest of the suspension was filtered through a syringe filter (0.22 μm, Millipore, Germany, GTBP), and the filter with the solids was placed in an empty serum vial, flushed with $N_2$ gas, and transferred back into the glovebox in order to prevent further oxidation. Inside the glovebox, the solids from the filter were resuspended in anoxic buffer (pH 7 MOPS, 25 mM). The suspension was then anoxically freeze-dried and preserved for spectroscopic analyses.

Similar to the complexation experiments, we set up POM-free and Fe(II)-free controls. Additionally, we prepared one set of reactors (duplicate) in order to track the oxidation of uncomplexed Fe(II) at pH 7. The concentration of Fe(II) in the POM-free oxidation reactors was set to 0.5 mM based on the mass of Fe(II) expected to be complexed by the POM based on the complexation results (Section 3.1). A small volume of Fe(II) stock solution was added to serum vials inside the glovebox, closed with butyl stoppers, and crimp-sealed. The vials were then brought outside the glovebox and opened, and oxic buffer (pH 7 MOPS, 25 mM) was added to the vials. The vials were then closed, crimp-sealed, and placed in a rolling shaker. The reactors were sacrificially sampled at time points similar to those of the Fe-POM reactors above.

In addition to the kinetic experiments at pH 7, we tested the oxidation of Fe(II)-complexed by POM at pH 5.5 after 20.5 h. Similar to the procedure above, we prepared anoxic Fe-POM at pH 5.5 inside the glovebox and exposed it to oxic buffer (pH 5.5 MES, 25 mM). After 20.5 h, we separated the solids from the aqueous phase by syringe filtration (0.22 μm, Millipore, Germany, GTBP), brought them into the glovebox, and resuspended them in anoxic buffer (pH 5.5 MES, 25 mM) to prevent further oxidation. The suspension was then anoxically freeze-dried and preserved for spectroscopic analyses. We set up corresponding POM-free reactors at pH 5.5 to determine the oxidation of uncomplexed Fe(II) after 20.5 h.

**2.6. Exposure of POM-Complexed Fe after Oxidation to Aqueous Fe(II).** To simulate anoxic, reducing conditions again after oxidation, we exposed oxidized Fe-POM to aqueous Fe(II). A secondary aim of this experiment was to test the reversibility of electron transfer after oxidation. We first reacted POM (1 g/L) with aqueous Fe(II) (1 mM) at pH 7 in triplicate reactors, as described in the complexation experiments above. After 24 h of reaction, we separated the Fe-POM from the aqueous phase by filtration (0.22 μm syringe filters, Millipore, Germany, GTBP) and exposed it to oxic buffer (pH 7 MOPS, 25 mM) as in the oxidation experiments above. We allowed oxidation to proceed for 24 h, after which we separated the oxidized Fe-POM by filtration and freeze-dried it. The freeze-dried oxidized Fe-POM was then transferred back into the glovebox. We then set up triplicate reactors in the glovebox by adding a predetermined volume of buffer (pH 7 MOPS, 25 mM) to the oxidized Fe-POM (1 g/L) and mixing on a rolling shaker (60 rpm) for 1 h. We then added a small volume of Fe(II) stock solution such that the aqueous Fe(II) concentration was 1 mM. After 24 h of mixing, we filtered an aliquot (≈0.4 mL) of the reactor suspension using a syringe filter (0.45 μm, Fisher Scientific, Germany, PTFE). The concentrations of aqueous Fe(II) and Fe(III) were measured using the ferrozine method.[49] The rest of the suspension was filtered (0.22 μm, Millipore, Germany, GTBP), and the solids were resuspended in buffer (pH 7, 25 mM MOPS) and


https://doi.org/10.1021/acsearthspacechem.3c00288
ACS Earth Space Chem. XXXX, XXX, XXX−XXX

anoxically freeze-dried. Samples were then prepared for XAS analyses.

**2.7. Spectroscopic Analyses.** *2.7.1. X-ray Absorption Spectroscopy (XAS).* Samples were analyzed by Fe *K*-edge (7112 eV) XAS at the XAFS beamline of ELETTRA (Trieste, Italy) and the SAMBA beamline of SOLEIL (Saint-Aubin, France). Freeze-dried solid samples were homogenized inside the glovebox manually with a mortar and pestle. The samples were then pressed into 7 mm (diameter) pellets and sealed with Kapton tape. At ELETTRA, transmission spectra were recorded at 80 K using a liquid $N_2$ cryostat. The monochromator (Si(111)) was calibrated to the first derivative maximum of the *K*-edge absorption spectrum of a metallic Fe foil (7112 eV). Higher beam harmonics were eliminated by detuning the monochromator by 30%. Two to four scans were collected and merged per sample. At SAMBA, transmission spectra were collected in continuous scan mode at 20 K using a liquid He cryostat with the monochromator (Si(220)) calibrated to the first derivative maximum of the *K*-edge absorption spectrum of a metallic Fe foil (7112 eV). Higher harmonics in the beam were eliminated via two Pd-coated mirrors. For each sample, 6 to 14 scans were collected and merged.

All spectra were energy calibrated, pre-edge subtracted, and post-edge normalized using Athena.[50] We analyzed the XANES (X-ray absorption near edge structure) region using linear combination fitting (LCF) to determine the Fe redox state using the references Fe(II)-citrate, Fe(III)-citrate, and ferrihydrite. For each sample, either Fe(III)-citrate or ferrihydrite were used as the Fe(III) reference, depending on the shape of the spectra. The LCF analyses were conducted over an energy range of −20 to 30 eV ($E-E_0$), where the $E_0$ values of the sample and reference spectra are defined as the maximum in the first XANES derivative. We analyzed the $k^3$-weighted EXAFS (extended X-ray absorption fine structure) spectra using LCF over a *k*-range of 2 to 11 $Å^{-1}$. Here, we used Fe(II)-EDA (ethylenediamine), Fe(II)-catechol, Fe(II)-EDTA (ethylenediaminetetraacetic acid), Fe(II)-mercaptoethanol, and Fe(II)-citrate as the Fe(II)-organic references and Fe(III)-catechol and Fe(III)-citrate as the Fe(III)-organic references to include a range of possible binding ligands. Ferrihydrite was also included as a reference. For EXAFS LCF, the $E_0$ values of the sample and reference spectra were set to 7128 eV. The EXAFS best fit was chosen based on a combinatorics approach. All 8 references were initially included in combinatorics, and final fits were chosen based on a criterion of a minimum 10% improvement in the *R*-factor.[51] During the fit, the components were constrained to values between 0 and 100%, and no constraints were applied on the sum of the components. A component was included only if its contribution was >5%. The resulting initial fit fractions (100 ± 14%) were later recalculated to 100%.

*2.7.2. Mössbauer Spectroscopy.* We analyzed selected samples with $^{57}$Fe Mössbauer spectroscopy: (i) the solid phase after reaction of POM with aqueous Fe(II) at pH 7 for 27 h and (ii) the solid phase after exposure of Fe-POM to $O_2$ at pH 7 for 20.5 h. After freeze-drying, samples were homogenized inside the glovebox. The sample powders were then loaded into Plexiglas holders (area of 1 $cm^2$), forming a disc. Holders were inserted into a closed-cycle exchange gas cryostat (Janis Cryogenics, USA) under a backflow of He to minimize exposure to air. Spectra were collected at 77 and 5 K using a constant acceleration drive system (WissEL, Germany) in transmission mode with a $^{57}$Co source in an Rh matrix. All spectra were calibrated against a 7 $\mu$m thick $\alpha$-$^{57}$Fe foil that was measured at room temperature. Analysis was carried out using Recoil (University of Ottawa, Canada) and the Voigt-based fitting (VBF) routine.[52] The half width at half-maximum (HWHM) was constrained to 0.123 mm/s during fitting.

## 3. RESULTS AND DISCUSSION

**3.1. Complexation of Fe(II) by POM.** We first determined the timescale of complexation of Fe(II) by exposing POM to aqueous Fe(II) at pH 7 for 27 h and measuring the change in aqueous Fe(II) over time. Upon exposure to POM, the aqueous Fe(II) decreased rapidly from 926 ± 43 $\mu$M (mean ± standard deviation) to 250 ± 9 $\mu$M over 5.5 h, and stayed constant thereafter (Figure S3). At the end of 27 h, the aqueous Fe(II) concentration was 268 ± 8 $\mu$M, corresponding to an Fe(II) uptake of 37.6 ± 1.5 mg Fe·$g^{-1}$ POM. For all subsequent complexation experiments, we chose the reaction time as 24 h in order to ensure that bulk aqueous equilibrium was achieved. The mass of Fe complexed by POM at lower pH values: 18.9 ± 1.2 mg Fe·$g^{-1}$ POM at pH 4.5 and 28.4 ± 1.3 mg Fe·$g^{-1}$ POM at pH 5.5. The increase in the mass of complexed Fe with pH is consistent with the protonation−deprotonation behavior of carboxyl and phenol groups within POM that are expected to act as binding sites for Fe:[13,53] at lower pH values, a larger proportion of carboxyl and phenol groups are expected to be protonated, resulting in fewer binding sites for Fe.[54,55] In contrast, at pH 7, a higher proportion of carboxyl and phenol groups is expected to be deprotonated, resulting in a higher affinity for Fe.

The range in the mass of POM-complexed Fe measured here (18.9 ± 1.2 mg Fe·$g^{-1}$ POM to 37.6 ± 1.5 mg Fe·$g^{-1}$ POM, corresponding to 0.74 ± 0.05 to 1.48 ± 0.06 mmol Fe·$g^{-1}$ C) is substantially lower than the Fe complexation capacities reported in previous studies on DOM and soil organic matter. Since this is the only study that directly tested Fe complexation by POM to our knowledge, we compared our results to (i) Fe complexed by DOM analogues, specifically humic and fulvic acids, and (ii) Fe content in organic-rich soils. The mass of POM-complexed Fe measured here is lower than the maximum capacities reported at pH 5 for humic acids (45 mmol Fe·$g^{-1}$ C) and fulvic acids (380 mmol Fe·$g^{-1}$ C).[56] There are likely two reasons for the lower extent of complexation of Fe by POM than by DOM analogues such as humic and fulvic acids. First, the carboxyl and phenol groups that act as binding sites for Fe may be fewer in POM than in humic and fulvic acids. The carboxyl content of humic and fulvic acids has been reported as 7.1 to 12.4 mequiv·$g^{-1}$ C and the phenolic content as 0.8 to 4.2 mequiv·$g^{-1}$ C.[57,58] Studies on the carboxyl and phenolic content of POM are few; one early study of 17 organic-rich soils that also included peat reported carboxyl contents of 0.4 to 1.4 mequiv·$g^{-1}$ C and phenolic contents of 2.6 to 3.7 mequiv·$g^{-1}$ C,[59] while another study measured 3.0−3.3 mequiv·$g^{-1}$ organic matter carboxyl groups and 1.8−2.0 mequiv·$g^{-1}$ organic matter phenolic groups.[60] Thus, the lower carboxyl and phenol contents of peat POM may have resulted in a lower level of Fe complexation by POM. The second possible reason for the lower level of complexation by POM as compared to DOM may be physical accessibility. The binding groups on POM may be less accessible to Fe as the POM is $\mu$m-sized (Figure S2),[46] while DOM may form nm-sized assemblies.[61,62] The values measured in our study were similar to those reported by


https://doi.org/10.1021/acsearthspacechem.3c00288
ACS Earth Space Chem. XXXX, XXX, XXX−XXX

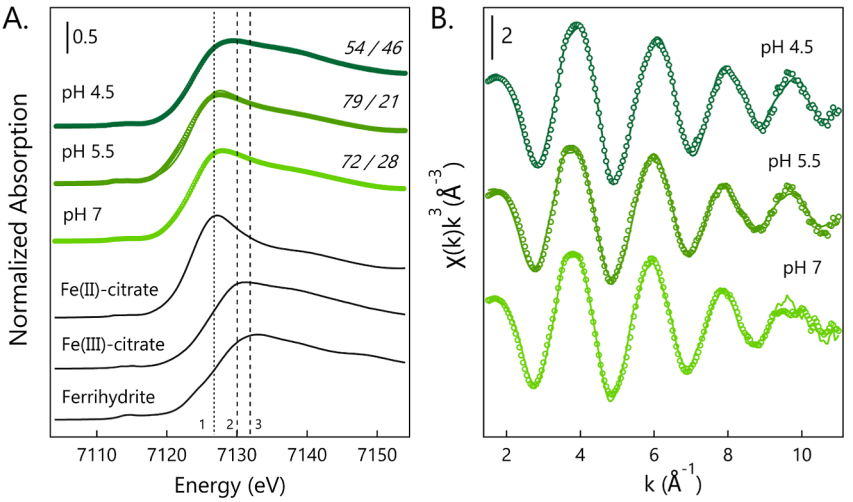


**Figure 1.** (A.) Normalized Fe K-edge XANES spectra and linear combination fits of Fe-POM (pH 4.5, 5.5, and 7) under anoxic conditions, as shown in green. Circular markers denote the experimental data and the solid lines denote the fits. Standards [Fe(II)-citrate, Fe(III)-citrate, and ferrihydrite, pH 7] used for linear combination fitting of the XANES region are in black lines. The dotted line (1) denotes the maximum absorption value of the Fe(II)-citrate reference and the dashed lines (2 and 3) denote the maximum absorption values of the Fe(III)-citrate and ferrihydrite references, respectively. Lines are shown for qualitative comparison with the maximum absorptions of the sample spectra. Numbers above each spectrum denote the fit fraction of Fe(II)/Fe(III) as percentages (fit results are given in Supporting Information, Table S1). (B) $k^3$-Weighted Fe *K*-edge EXAFS spectra of the anoxic Fe-POM phases (pH 4.5, 5.5, and 7) with their linear combination fits. Experimental data are shown as circular markers and fits are shown as solid lines. Spectra were fit within the range of $k$ = 2 to 11 Å$^{-1}$. Fit results are given in Table 1.

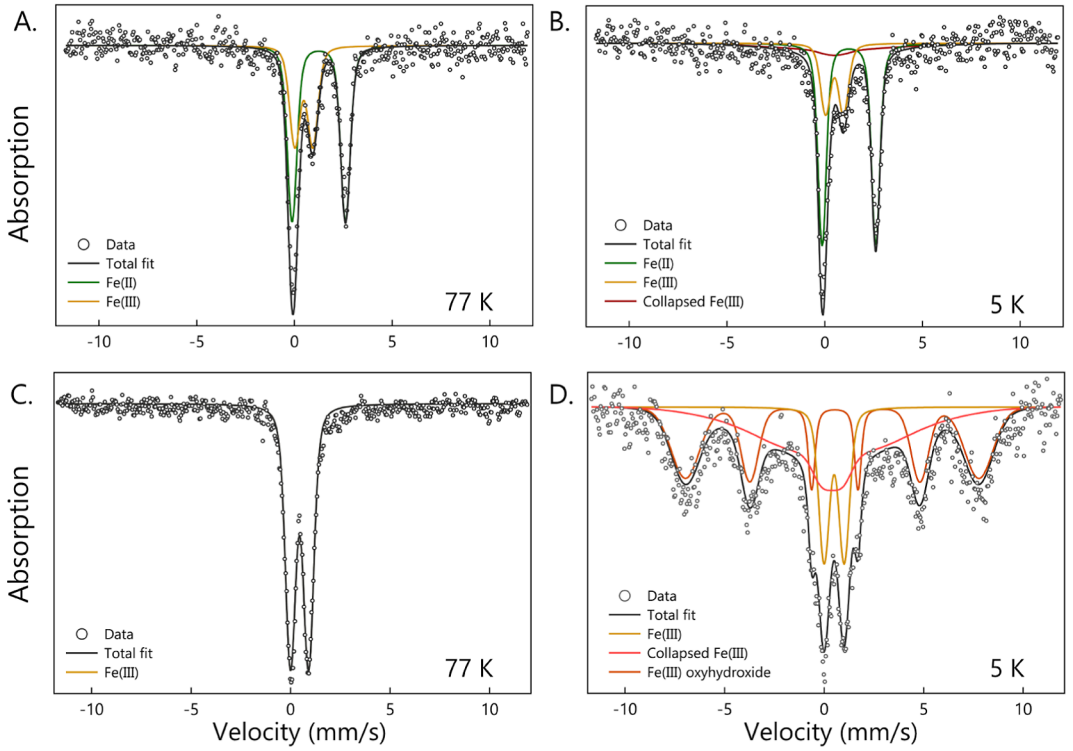


**Figure 2.** $^{57}$Fe Mössbauer spectra of Fe-POM under anoxic conditions (A,B) and after exposure to oxic conditions for 20.5 h (C,D) at pH 7. Spectra were collected at 77 (A,C) and 5 K (B,D). The markers denote the collected data, the colored solid lines denote the phases used for spectral fitting, and the black solid line denotes the total fit. Detailed fitting parameters are given in Table S2.

Catrouillet et al.[54] [up to 1.1 mmol of Fe·g$^{-1}$ C for Fe(II) binding to humic acids] at pH 5.9. However, that study used substantially lower Fe(II) concentrations (<100 $\mu$M) and acknowledged that saturation of binding sites had not been reached at the experimental concentrations. In contrast, our kinetic data at pH 7 indicate that all the possible binding sites had been saturated with Fe(II), as evidenced by stable aqueous Fe(II) concentrations after 5.5 h of reaction (Figure S3).

The mass of Fe complexed by POM was similar to the Fe content reported for organic-rich soils. Using pyrophosphate-based treatments targeting organic matter complexed-Fe, Karlsson et al. reported 0.09 to 0.55 mmol of Fe·g$^{-1}$ C in organic-rich forest soils (based on 39 to 108 mmol of Fe·kg$^{-1}$


https://doi.org/10.1021/acsearthspacechem.3c00288
ACS Earth Space Chem. XXXX, XXX, XXX−XXX

peat).[39] Two studies focusing specifically on peatlands[40,41] reported 0.15 to 0.5 mmol Fe·g$^{-1}$ C using the same pyrophosphate approach, consistent with the values observed in our work. The mass of POM-complexed Fe in organic-rich soils is at the lower end of the range observed in our laboratory study, likely due to the milled POM which may have increased the physical accessibility of Fe binding groups.

*3.1.1. Complexation with POM Oxidizes Fe(II) under Anoxic Conditions.* To determine the Fe redox state in Fe-POM, we first used the XANES region of the Fe *K*-edge XAS spectra. The energy of maximum absorption of the Fe-POM samples was 7128−7130 eV (Figure 1A), comparable to the maximum absorption energies of the standards Fe(II) citrate (7127 eV), Fe(III) citrate (7131 eV), and ferrihydrite (7133 eV). Upon linear combination fitting of the XANES region, the Fe-POM samples were found to contain both Fe(II) and Fe(III). The fractions of Fe(II) and Fe(III) were similar at pH 7 and pH 5.5: 72% Fe(II) and 28% Fe(III) at pH 7 and 79% Fe(II) and 21% Fe(III) at pH 5.5 (fit results given in Supporting Information, Table S1). At pH 4.5, the fraction of Fe(III) was substantially higher (46%), with the corresponding Fe(II) fraction as 54%. The results of XANES LCF were supported by the results of Mössbauer spectroscopy of the pH 7 Fe-POM sample (Figure 2A). At 77 K, the Mössbauer spectrum exhibited two clear doublets with parameters corresponding to Fe(II) (CS = 1.25 mm/s, QS = 2.72 mm/s) and Fe(III) (CS = 0.48 mm/s, QS = 0.92 mm/s).[63] Based on spectral fitting, we observed 62% Fe(II) and 37% Fe(III) (Table S2). The small difference in the Fe(III) fraction between the results of XANES fitting and Mössbauer spectrum fitting may be due to the lower quality of the Mössbauer spectrum, which may have resulted from the high organic matter content. Together, the results of XANES and Mössbauer spectroscopy indicate that part of the complexed Fe(II) underwent oxidation upon reaction with POM under anoxic conditions.

To test if oxidation of POM-complexed Fe(II) occurred due to trace oxygen in the experimental setup, we measured aqueous Fe(II) and Fe(III) concentrations in control reactors, to which we added Fe(II) (1 mM) and no POM. At all pH values, we observed no substantial decrease in Fe(II). The final Fe(II) concentrations in the control reactors were 1.01 ± 0.02 mM at pH 4.5, 0.92 ± 0.03 mM at pH 5.5, and 1.10 ± 0.03 mM at pH 7. No Fe(III) was detected in the control reactors at any pH. The constant Fe(II) concentrations in the absence of POM indicate that no oxygen was present in the experimental setup; thus, the oxidation of POM-complexed Fe(II) can be attributed to POM.

The anoxic partial oxidation of Fe(II) in the presence of POM may be due to electron transfer from Fe(II) to POM. We first examine the possible electron transfer from Fe(II). Complexation of Fe(II) by POM may alter its reduction potential ($E_H$), similar to the change in $E_H$ upon complexation with organic ligands.[11,64,65] For example, the standard reduction potential ($E^0_H$) of Fe(III)-acetate/Fe(II)-acetate is 0.63 V,[21] while the $E^0_H$ of uncomplexed Fe(III)/Fe(II) is 0.77 V.[66] A recent study showed that at redox potentials at which uncomplexed Fe(II) was observed to be stable (e.g., 0.1 V at pH 7), certain Fe(II) complexes [Fe(II)-citrate and Fe(II)-NTA] were observed to be partially oxidized.[21] Direct evidence of Fe(II) oxidation by DOM was given by Daugherty et al., who observed 40% oxidation of Fe(II) by untreated leonardite humic acid (LHA) under anoxic conditions.[24] Further support for the anoxic oxidation of complexed Fe(II) is given by Bhattacharyya et al., who reacted Fe(II) with the amino acids cysteine, arginine, and histidine and observed that 20−38% of Fe(II) bound to these amino groups was oxidized under anoxic conditions in less than 30 min.[67] Conversely, the authors also observed that after the reaction of Fe(III) with cysteine and arginine, a substantial fraction of the Fe(III) was reduced (80 and 14%, respectively), indicating that this electron transfer process was driven by the $E_H$ of the Fe(III)-amino acid/Fe(II)-amino acid redox couple. These past reports of electron transfer from Fe(II) in the presence of certain organic compounds may be translatable to our experimental system, suggesting that complexation by POM altered the redox potential of Fe(II)/Fe(III) and made oxidation thermodynamically favorable.

We then consider the suitability of the POM as an electron acceptor. DOM has been shown to reversibly accept electrons from a variety of electron donors.[48,65,68,69] Within DOM, quinone groups have been hypothesized to accept electrons, thereby forming hydroquinones.[70] This electron transfer has been observed to take place over a large range in $E_H$ values (−0.4 to 0.1 V at pH 7),[69] resulting in a large overlap between major redox couples in the environment and DOM $E_H$ values.[48] While the majority of previous work has focused on DOM, the redox properties of POM have only recently been quantified.[46,71,72] We compared the number of electrons that could theoretically be transferred to the POM during Fe(II) oxidation in our experimental system to its electron accepting capacity (EAC). The number of electrons transferred ranged from 0.23 to 0.41 mmol of $e^-$·g$^{-1}$ C (full calculations given in Table S3). This range is similar to the range in EAC of POM at pH 7 (0.48 to 0.95 mmol $e^-$·g$^{-1}$ C)[46] and slightly lower than the EAC of peat DOM at pH 7 (1.06 to 1.94 mmol $e^-$·g$^{-1}$ C).[73] The electron balance calculation here indicates that the electrons transferred during Fe(II) oxidation could, in principle, be accepted by POM.

The oxidation of Fe(II) was substantially higher at pH 4.5 (46%) relative to pH 5.5 and pH 7 (28 and 21%, respectively). One possible explanation for this difference is the effect of pH on electron transfer to quinone groups within POM. Quinone reduction is a two-electron and two-proton process at circumneutral to acidic pHs.[68,74] Therefore, quinone reduction is expected to be thermodynamically favored under lower pH conditions, resulting in more extensive electron transfer to POM at pH 4.5 relative to pH 5.5 and pH 7. It is, however, unclear why the oxidation at pH 5.5 was not higher than that at pH 7. The $E_H$ distribution of electron-accepting groups in POM and their pH dependence warrant further research.

We exclude the possibility that reactive oxygen species (ROS) were formed in the oxidized part of Fe(II) based on two lines of reasoning. First, we conducted all complexation experiments as well as sample preparation for spectroscopic analyses under anoxic conditions. No oxidation of Fe(II) was observed in the POM-free control reactors, indicating that anoxic conditions were maintained during the complexation. The XAS and Mössbauer spectroscopy analyses were performed on Fe-POM collected from separate experiments, indicating that the oxidation was systematic and unlikely to be caused by experimental error. Further, a previous study has shown that partial (90%) deoxygenation of buffer solutions is sufficient to inhibit the formation of ROS.[75] In our study, the glovebox atmosphere contained less than 0.01% of atmospheric oxygen levels at all times and all solutions had been sparged


https://doi.org/10.1021/acsearthspacechem.3c00288
ACS Earth Space Chem. XXXX, XXX, XXX−XXX

**Table 1. Linear Combination Fitting Results of Fe *K*-Edge EXAFS Spectra of POM-Complexed Fe at pH 4.5, 5.5, and 7 under Anoxic Conditions over the Course of Exposure to Oxic Conditions at pH 5.5 and 7, and after Exposure of the Oxidized Fe-POM to Aqueous Fe(II) at pH 7 under Anoxic Conditions**

| Sample | Fe(II) species (%)[a] | | | | Fe(III) species (%) | | | NSSR[b] (%) | red. $\chi^2$[c] |
|---|---|---|---|---|---|---|---|---|---|
| | Fe(II)-catechol | Fe(II)-EDTA | Fe(II)-mercaptoethanol | Fe(II)-citrate | Fe(III)-catechol[d] | Fe(III)-citrate[d] | Ferrihydrite | | |
| Complexation | | | | | | | | | |
| pH 4.5 | 28 | 7 | | 12 | | 35 | 18 | 1.4 | 0.047 |
| pH 5.5 | 34 | 18 | | 10 | | 23 | 15 | 2.1 | 0.048 |
| pH 7 | 36 | 14 | 7 | 11 | | 19 | 13 | 1.8 | 0.056 |
| Exposure of Fe-POM to Oxic Conditions at pH 7 | | | | | | | | | |
| $t$ = 5 min | | 8 | | | 15 | 25 | 52 | 2.5 | 0.081 |
| $t$ = 20 min | | | | | | 40 | 60 | 3.2 | 0.110 |
| $t$ = 2 h | | | | | 20 | | 80 | 3.3 | 0.128 |
| $t$ = 20.5 h | | | | | 17 | | 83 | 6.7 | 0.300 |
| Exposure of Fe-POM to Oxic Conditions at pH 5.5 | | | | | | | | | |
| $t$ = 20.5 h | | | | | 45 | | 55 | 6.7 | 0.183 |
| Exposure of Oxidized Fe-POM to Aqueous Fe(II) under Anoxic Conditions at pH 7 | | | | | | | | | |
| $t$ = 24 h | | 12 | 11 | | | 24 | 53 | 1.1 | 0.031 |

[a]The reference spectrum for Fe(II)-EDA was offered during fitting but was not matched in any of the fits. [b]NSSR: normalized sum of squared residuals $\left(\frac{\Sigma_i(\text{data}_i - \text{fit}_i)^2}{\Sigma_i \text{data}^2} \cdot 100\right)$. [c]Reduced $\chi^2 = \frac{N_{idp}}{N_{pts}} \cdot \Sigma_i \cdot \frac{(\text{data}_i - \text{fit}_i)^2}{\sigma_i^2} \cdot (N_{idp} - N_{var})^{-1}$. $N_{idp}$, $N_{pts}$, and $N_{var}$ are the number of independent points (18), the total number of data points (181), and the number of fit variables, respectively (2–6). [d]Note that the reference spectra for Fe(III)-citrate and Fe(III)-catechol (Supporting Information, Figure S4) are similar, leading to possible ambiguities in assigning relative proportions of these two references in linear combination fitting.

with $N_2$ for 2 h prior to being moved into the glovebox. As a result, it is highly unlikely that ROS were formed and were responsible for Fe(II) oxidation.

We also considered the possibility that anoxic Fe(II) oxidation in the presence of POM was due to microorganisms in the POM. Although we did not sterilize the POM as we wanted to avoid changes in the POM composition, we expect that processing the POM decreased the likelihood of an active Fe(II)-oxidizing microbial community. The POM was commercially obtained, dried in air, and milled before use in the experiments. During drying, the POM was exposed to air for 48 h, and anoxic conditions were not maintained. We expect that the lack of water and long exposure to $O_2$ in the air minimized the likelihood of an Fe(II)-oxidizing microbial community active enough to oxidize 21–46% Fe(II) in 24 h. Further, there is no clear electron acceptor for anaerobic Fe(II) oxidation by microorganisms in our system. The steps taken to establish anoxic conditions in the experimental system (e.g., bubbling all solutions for 2 h with $N_2$) preclude microaerophilic Fe(II) oxidation. No nitrate was present, excluding the possibility of nitrate-dependent Fe(II) oxidation. All of our experiments were conducted in the dark; therefore, no phototrophic Fe(II) oxidation was expected to occur. The only possible electron acceptor is the POM itself. Although we speculate here (and in our previous work[46,76]) that POM may act as an electron acceptor, there have been no reports of Fe(II) oxidation by microorganisms coupled to POM reduction so far. Hence, we expect that the oxidation of Fe(II) upon complexation with POM observed in our study is an abiotic process.

The anoxic oxidation of Fe(II) by POM has implications for Fe redox behavior in wetlands. Based on our results, the infiltration of molecular $O_2$ is not necessary for the oxidation of POM-complexed Fe(II) to Fe(III). Ferrous Fe formed under reducing conditions may be complexed by POM and partially oxidized (21–46%) to Fe(III), resulting in a mixed Fe(II)/Fe(III) phase, even in the absence of $O_2$. These mixed Fe(II)/Fe(III) phases may fuel further Fe cycling by providing a pool of Fe(III). Measurements of solid-phase Fe(II) in wetlands as an indicator of microbial Fe(III) reduction may therefore be underestimates, as part of the Fe(II) produced during reduction is likely abiotically oxidized to Fe(III) upon complexation with POM. Conversely, the presence of Fe(III) in such systems may not be an unambiguous indicator of past oxygen or of microbial oxidation. Additionally, the redox reactivity of Fe(II) toward pollutants may be enhanced due to the presence of small quantities of Fe(III).

*3.1.2. Speciation of POM complexed-Fe under Anoxic Conditions.* The EXAFS region of the Fe *K*-edge spectra of all Fe-POM samples could be fit with Fe(II)-organic, Fe(III)-organic, and ferrihydrite reference spectra: Fe(II)-EDTA (8–18%), Fe(II)-catechol (28–36%), Fe(III)-citrate (19–35%), and ferrihydrite (15–21%) (Figure 1B, Table 1). In one sample (pH 7), the best fit resulted in a 7% contribution of Fe(II)-mercaptoethanol. The lack of Fe(II)-EDA in the fits is consistent with the affinity of Fe toward carboxyl and phenol groups[13,24] that are present in citrate, EDTA, and catechol but absent in EDA. In our spectra, the assignment of contributions of Fe(III)-citrate and Fe(III)-catechol may be ambiguous because the reference spectra for Fe(III)-citrate and Fe(III)-catechol were quite similar (Figure S4). Therefore, we collectively refer to the relative proportions of species modeled as these two reference spectra as "Fe(III)-organics". The small fraction of ferrihydrite in the fits was unexpected as the presence of high quantities of organic matter has been shown to inhibit mineral formation.[1,77,78]

We further investigated this ferrihydrite-like phase by analyzing the Mössbauer spectrum of pH 7 Fe-POM, collected at 5 K (Figure 2B). At this temperature, ferrihydrite is expected to exhibit a magnetically ordered sextet, which would be absent in the 77 K spectrum discussed above.[1,63,79] The spectrum collected at 5 K exhibited one Fe(II) doublet, one Fe(III)


https://doi.org/10.1021/acsearthspacechem.3c00288
ACS Earth Space Chem. XXXX, XXX, XXX−XXX

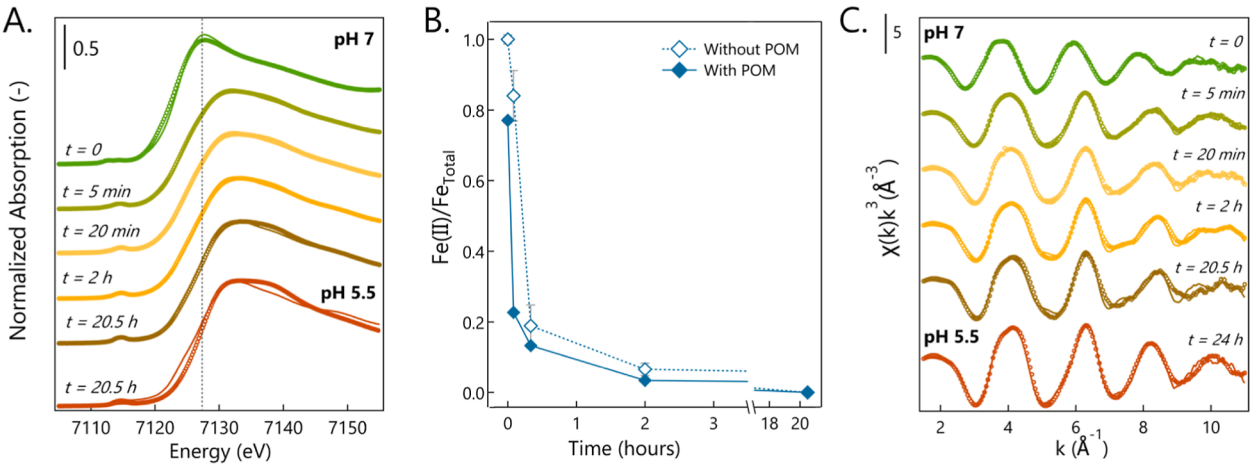


**Figure 3.** Iron redox state and speciation in Fe-POM phases over the course of exposure to oxygen. (A) Fe *K*-edge XANES spectra of Fe-POM phases after exposure to oxygen at pH 7 and pH 5.5 with their linear combination fits. Circular markers denote the experimental data and the solid lines denote the fits. The vertical dotted line denotes the maximum absorption value of the Fe-POM phase before exposure to oxic conditions for visual comparison with the spectra collected at later time points. (B) Fraction of Fe(II) [Fe(II)/Fe$_{total}$] in Fe-POM phases compared to the Fe(II) fraction in POM-free control experiments at pH 7. Markers denote the mean and the error bars denote the range of duplicate reactors in the POM-free experiments. In the POM reactors, the markers denote the Fe(II) fraction based on the LCF analysis of the XANES region of Fe *K*-edge spectra at each time point. (C) Fe *K*-edge $k^3$-weighted EXAFS spectra of Fe-POM phases after exposure to oxic conditions at pH 7 and pH 5.5 and their linear combination fits. Experimental data are shown with circular markers and fits are shown as solid lines. Spectra were fit within the range of $k$ = 2 to 11 Å$^{-1}$. Fitting results are listed in Table 1.

doublet, and a collapsed Fe(III) sextet (Figure 2B and Table S2). The doublets likely correspond to the Fe(II)-organic and Fe(III)-organic species which are not magnetically ordered and therefore are not expected to split into a sextet. The presence of the collapsed Fe(III) sextet (15%) and absence of an ordered sextet suggest that the phase modeled as ferrihydrite in the EXAFS LCF is likely a very poorly ordered Fe(III) (oxyhydr)oxide that is less crystalline than the ferrihydrite reference used in most mineralogical analyses. A similar collapsed Fe(III) sextet present in spectra collected at 5 K has been suggested to represent poorly/nanocrystalline Fe oxyhydroxides by other studies that investigated the oxidation of aqueous Fe(II) in the presence of organic matter.[25,32] Note that no Fe (oxyhydr)oxides of higher crystallinity, such as lepidocrocite or goethite, could be fit in the Mössbauer spectroscopy or XAS analyses.

Based on the XAS and Mössbauer spectroscopy analyses, we observed that the Fe bound to POM was composed of Fe(II)-organic phases, Fe(III)-organic phases, and a poorly crystalline, ferrihydrite-like mineral. The composition of these Fe-POM phases is similar to the Fe-organic phases observed in the environment, especially in wetlands that are water-saturated and therefore subject to anoxic conditions. Consistent with our results, Bhattacharyya et al. observed a mix of Fe(II) and Fe(III) phases in anoxic peats from peatlands in northern New York.[40] Based on EXAFS analysis, they observed that all of the Fe(II) present could be modeled as Fe(II)-organic complexes. The coexistence of Fe(II) and Fe(III) bound to organic ligands was also found in permafrost peatlands, especially in the soil layers with high organic matter content.[41] Thus, the Fe-POM phases observed in the environment may be formed by the complexation of Fe(II) by POM, followed by partial anoxic oxidation to Fe(III). Future work should focus on analyzing the specific functional groups of POM that bind Fe(II) using a correlational molecular spectroscopic technique such as scanning transmission X-ray microscopy (STXM) connected to the near edge X-ray absorption fine structure (NEXAFS) of Fe and carbon to identify the functional groups responsible for Fe(II) oxidation.

**3.2. Oxidation of POM-Complexed Fe(II) upon Exposure to Oxygen.** *3.2.1. Change in Fe Redox State during Exposure to Oxygen.* We investigated the oxidation of POM-complexed Fe upon exposure to oxygen ($O_2$) at pH 7 in order to simulate switches in the redox state. To determine the Fe redox state over the course of $O_2$ exposure, we analyzed the solid phase via Fe *K*-edge XAS. We chose this method as opposed to a wet chemical method such as acidification followed by a spectrophotometric assay because the presence of organic matter has been shown to affect the Fe redox state during acid extractions.[80] In the XANES region of the spectra, the position of the maximum absorption shifted to higher energies over time, indicating that Fe(II) was oxidized (Figure 3A). Based on LCF analysis, the Fe(II)/Fe$_{total}$ ratio was 0.77 at the start of the reaction, similar to the ratio observed upon complexation of Fe(II) by the POM under anoxic conditions (Section 3.1 above). The Fe(II)/Fe$_{total}$ ratio decreased rapidly thereafter, from 0.23 after 5 min to 0.03 at the end of 2 h (Figure 3B and Table S1). After 20.5 h of exposure to $O_2$, no Fe(II) remained. The results of the XANES fitting were supported by Mössbauer spectroscopy of the solid phase at the end of 20.5 h. The 77 K spectrum exhibited a single Fe(III) doublet (CS = 0.45 mm/s, QS = 0.91 mm/s), indicating complete oxidation (Figure 2C).

We compared the oxidation of Fe(II) complexed by POM with the oxidation of uncomplexed Fe(II) under the same conditions (pH 7 MOPS, 25 mM). We observed that the oxidation of uncomplexed Fe(II) was rapid, with a decrease in Fe(II)/Fe$_{total}$ from 1.00 at the beginning of the experiment to 0.84 after 5 min and 0.07 after 2 h of reaction (Figure 3B). The observed rapid oxidation was expected since Fe(II) is not stable in the presence of oxygen at a neutral pH.[1,66] Note here that we measured the Fe(II) and Fe(III) concentration in the uncomplexed Fe(II) control experiment using a spectrophotometric assay,[49] as (i) there was no interference from organic


https://doi.org/10.1021/acsearthspacechem.3c00288
ACS Earth Space Chem. XXXX, XXX, XXX−XXX

matter in Fe(II) quantification in these experiments, and (ii) there was little to no solid for XAS analysis for the initial time points.

In order to further test if complexation by POM could promote Fe(II) oxidation, we exposed Fe-POM to an $O_2$-containing buffer at pH 5.5. At this pH, the oxidation of Fe(II) is expected to be inhibited due to thermodynamic[24,66] and kinetic[81] limitations. The reduction potential ($E_H$) at which Fe(II) is stable is much higher (>0.5 V) at pH 5.5 relative to pH 7.[66] After the reaction of Fe-POM with $O_2$ for 20.5 h, we collected the solid phase and determined the Fe redox state using Fe *K*-edge XAS. Based on LCF analysis of the Fe *K*-edge XANES spectra, all of the Fe in the Fe-POM phase was Fe(III), i.e., complete oxidation had occurred (Figure 3A). In contrast to the POM-complexed Fe(II), the uncomplexed aqueous Fe(II) concentration did not change over the reaction period (497 ± 1 $\mu$M at $t$ = 0 to 484 ± 1 $\mu$M at $t$ = 20.5 h). Thus, complexation with POM promoted Fe(II) oxidation in the presence of dissolved $O_2$ at pH 5.5. As the kinetics of Fe(II) oxidation are pH-dependent, future studies should investigate the Fe(II) oxidation in the presence of POM over time at lower pHs. Collectively, our results suggest that complexation by POM likely promotes the oxidation of Fe(II) in the presence of $O_2$.

The observed oxidation of Fe(II) is the net result of several processes: direct oxidation by $O_2$ followed by the generation of ROS such as hydroxyl radicals, hydrogen peroxide, and superoxide, and subsequent oxidation by ROS.[82] These processes are partially counteracted by the back-reaction of superoxide with Fe(III), resulting in the reformation of Fe(II), which has been invoked to explain the persistence of Fe(II) under oxic conditions[24] and decreases in the rate of oxidation.[83] We observed no inhibition of Fe(II) oxidation upon POM complexation, contrary to the widely reported role of DOM as an inhibitor of Fe(II) oxidation. Our results specifically differ from those of Daugherty et al., who reduced LHA before reacting with Fe(II)[24] at pH 7. The prereduction step in Daugherty et al. likely resulted in an increase in the electron-donating capacity of the LHA. The reduced LHA may have promoted a back-reaction with the Fe(III) that resulted in the persistence of Fe(II). In our study, we did not prereduce the POM, thereby decreasing the likelihood of Fe(III) rereduction to Fe(II). Two additional factors may have resulted in the rapid oxidation of POM-complexed Fe(II). First, the presence of high quantities of organic matter has been shown to scavenge superoxide radicals.[83] Further, the reactivity of organically complexed Fe(III) toward the back-reaction with superoxide radicals is suppressed relative to uncomplexed Fe(III).[84] Hence, the high C/Fe ratios (≈20) in our experiments may have inhibited back-reaction of Fe(III) with superoxide. Second, oxidation of Fe(II) has been shown to be promoted by the presence of ferric phases (termed "heterogeneous oxidation") relative to Fe(II) oxidation in the absence of a ferric phase.[25,32] As there is a small fraction of Fe(III) phases (Fe(III)-OM, ferric (oxyhydr)oxide mineral similar to ferrhydrite) in the Fe-POM even under anoxic conditions, oxidation of Fe(II) may have proceeded heterogeneously.

*3.2.2. Speciation of Fe-POM over the Course of Oxidation.* Based on LCF analysis of the Fe *K*-edge EXAFS region, we observed a rapid decrease in the fraction of Fe(II)-organic phases coupled to an increase in the fraction of Fe(III)-organic phases as well as the ferrihydrite-like phase (Figure 3C and Table 1). By the end of 20.5 h, all the Fe was present in the form of Fe(III)-organics (17%) and a ferrihydrite-like mineral (83%). The fraction of Fe(III)-organics after exposure to $O_2$ for 20.5 h (17%) was similar to that in the Fe-POM under anoxic conditions (19%), suggesting that the Fe(III)-organic fraction was unaffected, while Fe(II)-organic bonds were broken to form the ferrihydrite-like mineral. We observed similar Fe speciation of Fe-POM exposed to oxygen at pH 5.5 for 24 h (red line, Figure 3C); all the Fe(II) was oxidized to Fe(III) in the form of Fe(III)-organic (45%) and a ferrihydrite-like mineral (55%). The higher fraction of Fe(III)-organics in the Fe-POM after exposure to $O_2$ at pH 5.5 relative to that at pH 7 suggests that the Fe(II)-organics were oxidized to Fe(III)-organics as well as the ferrihydrite-like mineral. The dominance of Fe(III) phases in the linear combination fits of the EXAFS region is consistent with the rapid oxidation based on the interpretation of the XANES region.

Complementary to Fe *K*-edge XAS, we also collected Mössbauer spectra of the pH 7 Fe-POM after 20.5 h of $O_2$ exposure (Figure 2C,D). The presence of an Fe(III) doublet and the lack of an ordered sextet indicated that no crystalline Fe(III) (oxyhydr)oxides such as goethite were formed (Figure 2C). This result was consistent with our EXAFS fitting results (Table 1). The spectrum collected at 5 K exhibited several features indicative of Fe(III) phases. The spectrum was fit with one Fe(III) doublet (19%), one Fe(III) sextet (41%), and one collapsed sextet (40%) (Table S1). The Fe(III) doublet (CS = 0.5 mm/s and QS = 1.01 mm/s) likely represented the Fe(III)-organic phases as they do not magnetically order even at 5 K. The ordered Fe(III) sextet exhibited parameters (CS = 0.47 mm/s, $\epsilon$ = −0.07 mm/s, and H = 45.7 T) similar to those of ferrihydrite,[63] although with broadened peaks, which may indicate structural disorder.[1,63] A collapsed sextet (CS = 0.4 mm/s, $\epsilon$ = 0 mm/s, and H = 21.7 T) was necessary to explain the spectrum; this feature may represent a very poorly ordered Fe(III) oxyhydroxide.[32] Such poorly crystalline Fe oxyhydroxide phases, also referred to as "very short-range-ordered" (SRO) phases, have been observed to form during the oxidation of Fe(II) in the presence of DOM analogues (such as SRFA)[25] and organic-rich soils.[32] The results of these analyses indicate that the oxidation of Fe-POM results primarily in Fe(III) (oxyhydr)oxides of low and varying crystallinity with a small proportion of Fe(III)-organic matter phases. The low crystallinity of these species suggests that they may be thermodynamically favorable electron acceptors for Fe(III)-reducing microorganisms during later reducing periods. The enhanced bioavailability of poorly crystalline minerals formed by oxidation in organic-rich soils has been previously reported,[33] supporting the likelihood that the products of oxidation of POM-complexed Fe(II) will be readily reducible.

**3.3. Exposure of Oxidized Fe-POM to Aqueous Fe(II).** We exposed oxidized Fe-POM to aqueous Fe(II) for two purposes: (i) to simulate an increase in the water table that may lead to the re-establishment of anoxic, reducing conditions after an oxic period, and (ii) to determine whether the electron transfer between Fe(II) and POM was reversible. Upon the reaction of oxidized Fe-POM [Fe(III)-POM] with aqueous Fe(II) at pH 7, we observed uptake of Fe(II) by POM from the solution, which corresponded to an additional 29.2 mg of Fe·g$^{-1}$ POM. This additional uptake of Fe(II) may be due to binding sites within POM that were vacated during the oxidation of Fe-POM. Upon complexation of Fe(II) by POM, organic groups (such carboxyl and phenols) bound Fe. After


https://doi.org/10.1021/acsearthspacechem.3c00288
ACS Earth Space Chem. XXXX, XXX, XXX−XXX

exposure to $O_2$, we observed that all the Fe(II) (present as Fe(II)-organics) was oxidized (Section 3.2), partially leading to the formation of a ferrihydrite-like mineral. In order to form the Fe−Fe bonds in such a ferric (oxyhydr)oxide mineral, the Fe-organic bonds were likely broken, making these binding sites available for further complexation of the aqueous Fe(II) that was added in this experiment. The proportion of Fe(II) [Fe(II)/$Fe_{total}$ ratio] of the reacted Fe-POM was 28% based on LCF analysis of the XANES region of Fe *K*-edge XAS spectra (Figure S5A and Table S1). Mass balance calculations of the Fe(II) and Fe(III) contents of the unreacted and reacted Fe-POM indicated that the part of newly added Fe(II) that was taken up from the solution had been oxidized (Table S3). Based on the additional uptake of Fe(II) and its subsequent oxidation, we rejected the hypothesis that electron transfer between aqueous Fe(II) and POM was reversible. If electron transfer had indeed been reversible, then the exposure of Fe(III)-POM to aqueous Fe(II) should result in the reduction of Fe(III) to Fe(II), with Fe(III) fractions similar to those after the initial complexation (Section 3.1). One possible reason for the lack of reversibility is that redox equilibrium was not established between the several species present in the system. The Fe(II) taken up by the solid may have sorbed onto Fe(III) (oxyhydr)oxides, participated in ligand exchange with POM-complexed Fe(III), and/or further complexed with Fe-binding groups on POM. Therefore, the possible species present include POM-complexed Fe(II), POM-complexed Fe(III), the Fe(III) (oxyhydr)oxides, Fe(II) sorbed to the (oxyhydr)-oxides, and aqueous Fe(II), which may not have reached redox equilibrium over experimental time scales (24 h). In our experimental system, we do not expect the Fe(III) (oxyhydr)-oxides to undergo Fe(II)-catalyzed transformation,[85] as the high organic carbon/iron ratios present in our system would likely inhibit such mineral transformation.[77,78,86]

To determine the species present in Fe-POM after exposure to aqueous Fe(II), we analyzed the EXAFS region of the Fe *K*-edge XAS spectra with linear combination fitting. The Fe-POM after reaction with Fe(II) contained Fe(II)-organics (23%), Fe(III)-organics (24%), and a ferrihydrite-like mineral (53%) (Table 1, Figure S5B). Mass balance calculations based on the EXAFS fitting and the total mass of solid-phase Fe showed that the mass of Fe(II)-organic phases and Fe(III)-organic phases increased, while the mass of the ferrihydrite-like mineral was unchanged (Supporting Information, Section S6). Thus, Fe(II) taken up during exposure of the oxidized Fe-POM to aqueous Fe(II) was likely mainly complexed by the POM and partially oxidized to Fe(III)-organics. These results suggest that redox oscillations may lead to the accumulation of Fe(II)-organics and Fe(III)-organics in reducing periods and the accumulation of ferrihydrite-like Fe(III) (oxyhydr)oxides in oxidizing periods.

## 4. CONCLUSIONS

In this work, we investigated the complexation of aqueous Fe(II) by POM under varying redox conditions. Under anoxic conditions, POM complexed 18.9 ± 1.2 to 37.6 ± 1.5 mg of $Fe{\cdot}g^{-1}$ POM over a pH range of 4.5 to 7. Although the carbon-normalized mass of Fe complexed by POM was lower than that reported for DOM complexation, we expect that complexation by POM plays a much larger role than by DOM in wetland soils because most organic carbon in these systems is present in particulate form. For example, >95% of organic carbon in ombrotrophic bogs occurs in particulate form.[35] Upon complexation by POM, part of Fe(II) was oxidized to Fe(III) under anoxic conditions, indicating that the reduction potential of POM-complexed Fe(III)/Fe(II) is different from that of uncomplexed Fe(III)/Fe(II) and Fe(III) oxide/Fe(II). This has several implications for microbial metabolism and pollutant turnover. First, the thermodynamic favorability of microbial Fe(II) oxidation may be affected if Fe(II) is complexed by POM, potentially promoting oxidation rates and/or extents. Second, POM-complexed Fe(II) may be an enhanced abiotic reductant of contaminants, as reported for Fe(II) complexed by small organic molecules.[22] In addition, oxidation part of the complexed Fe(II) may provide new Fe(III) species for microbial Fe(III)-reducing microorganisms without the need for molecular $O_2$. Spectroscopic analyses of the oxidation products indicated the presence of Fe(III)-organic phases and a very poorly crystalline, ferrihydrite-like mineral, both of which may be easily reduced by microorganisms.

Upon exposure to oxic conditions at pH 5.5 and 7, POM-complexed Fe(II) rapidly oxidized, indicating that complexation promoted Fe(II) oxidation. The oxidation products were a mixture of Fe(III)-organic phases and poorly crystalline Fe oxyhydroxides. These phases would likely be less thermodynamically stable than more crystalline Fe minerals present in the soil and would therefore be preferentially used as electron acceptors by Fe(III)-reducing microorganisms in subsequent anoxic periods, e.g., due to a later increase in the water table. The poorly crystalline Fe oxyhydroxides formed due to oxidation may also act as sorbents for nutrients (such as phosphate) and trace elements (such as metals). Collectively, our results indicate that complexation by POM likely plays a crucial role in the Fe redox cycle in wetland soils, affecting both abiotic and microbial processes.

## ■ ASSOCIATED CONTENT

### Supporting Information

The Supporting Information is available free of charge at https://pubs.acs.org/doi/10.1021/acsearthspacechem.3c00288.

> Detailed description of peat POM characterization methods, aqueous Fe(II) concentrations in the anoxic Fe(II) complexation experiments over time at pH 7, results of LCF analysis of Fe *K*-edge XANES, Mössbauer fitting parameters, EXAFS spectra of references used for LCF analysis of Fe *K*-edge XAS, calculations of theoretical number of electron transferred to POM and masses of Fe phases based on Fe *K*-edge XAS, and XANES and EXAFS spectra of oxidized Fe-POM exposed to aqueous Fe(II) under anoxic conditions at pH 7 (PDF)

## ■ AUTHOR INFORMATION


### Corresponding Author

**Prachi Joshi** − *Geomicrobiology, Department of Geosciences, University of Tübingen, 72076 Tübingen, Germany;* orcid.org/0000-0001-5954-0309; Email: prachi.joshi@uni-tuebingen.de

### Authors

**Laurel K. ThomasArrigo** − *Soil Chemistry Group, Institute of Biogeochemistry and Pollutant Dynamics, Department of Environmental Systems Science, ETH Zürich, CH-8092 Zürich, Switzerland; Environmental Chemistry Group,*




https://doi.org/10.1021/acsearthspacechem.3c00288
ACS Earth Space Chem. XXXX, XXX, XXX−XXX

*Institute of Chemistry, University of Neuchâtel, 2000 Neuchâtel, Switzerland;* orcid.org/0000-0002-6758-3760
**Dennis Sawwa** − *Geomicrobiology, Department of Geosciences, University of Tübingen, 72076 Tübingen, Germany*
**Lea Sauter** − *Geomicrobiology, Department of Geosciences, University of Tübingen, 72076 Tübingen, Germany*
**Andreas Kappler** − *Geomicrobiology, Department of Geosciences, University of Tübingen, 72076 Tübingen, Germany; Cluster of Excellence, EXC 2124: Controlling Microbes to Fight Infection, University of Tübingen, 72076 Tübingen, Germany;* orcid.org/0000-0002-3558-9500

Complete contact information is available at: https://pubs.acs.org/10.1021/acsearthspacechem.3c00288

### Notes

The authors declare no competing financial interest.

## ■ ACKNOWLEDGMENTS

We thank Yuge Bai for help with the elemental analysis of the POM, Biao Wan for the collection of FTIR spectra, and Nina Reimann, Hira Curcialo, Monica Terrazza, and Simon Ferlein for help with laboratory analyses. We also thank Muammar Mansor for the POM particle size distribution data. We acknowledge ELETTRA (proposal no. 20215103) and Soleil (proposal no. 20210970) for the provision of synchrotron radiation facilities and thank Danilo Oliviera de Souza (XAFS beamline, ELETTRA) and Gautier Landrot (SAMBA beamline, SOLEIL) for support during synchrotron XAS measurements. We are grateful to Thomas Borch for sharing the reference spectra for Fe(II)-organics and Fe(III)-organics. This research was funded by the German Research Foundation (DFG, KA 1736/66-1). A.K. acknowledges infrastructural support by the DFG under Germany's Excellence Strategy EXC 2124, project ID 390838134.

## ■ REFERENCES

(1) Cornell, R. M.; Schwertmann, U. *The Iron Oxides: Structure, Properties, Reactions, Occurences and Uses*; Wiley Online Books, 2003.
(2) Kappler, A.; Bryce, C.; Mansor, M.; Lueder, U.; Byrne, J. M.; Swanner, E. D. An evolving view on biogeochemical cycling of iron. *Nat. Rev. Microbiol.* **2021**, *19*, 360−374.
(3) Borch, T.; Kretzschmar, R.; Kappler, A.; Cappellen, P. V.; Ginder-Vogel, M.; Voegelin, A.; Campbell, K. Biogeochemical Redox Processes and their Impact on Contaminant Dynamics. *Environ. Sci. Technol.* **2010**, *44*, 15−23.
(4) Elsner, M.; Schwarzenbach, R. P.; Haderlein, S. B. Reactivity of Fe(II)-Bearing Minerals toward Reductive Transformation of Organic Contaminants. *Environ. Sci. Technol.* **2004**, *38*, 799−807.
(5) Hofstetter, T. B.; Heijman, C. G.; Haderlein, S. B.; Holliger, C.; Schwarzenbach, R. P. Complete Reduction of TNT and Other (Poly)nitroaromatic Compounds under Iron-Reducing Subsurface Conditions. *Environ. Sci. Technol.* **1999**, *33*, 1479−1487.
(6) Klausen, J.; Troeber, S. P.; Haderlein, S. B.; Schwarzenbach, R. P. Reduction of Substituted Nitrobenzenes by Fe(II) in Aqueous Mineral Suspensions. *Environ. Sci. Technol.* **1995**, *29*, 2396−2404.
(7) Wiatrowski, H. A.; Das, S.; Kukkadapu, R.; Ilton, E. S.; Barkay, T.; Yee, N. Reduction of Hg(II) to Hg(0) by Magnetite. *Environ. Sci. Technol.* **2009**, *43*, 5307−5313.
(8) Pedersen, H. D.; Postma, D.; Jakobsen, R. Release of arsenic associated with the reduction and transformation of iron oxides. *Geochim. Cosmochim. Acta* **2006**, *70*, 4116−4129.
(9) Wang, L.; Giammar, D. E. Effects of pH, dissolved oxygen, and aqueous ferrous iron on the adsorption of arsenic to lepidocrocite. *J. Colloid Interface Sci.* **2015**, *448*, 331−338.
(10) Kügler, S.; Cooper, R. E.; Wegner, C.-E.; Mohr, J. F.; Wichard, T.; Küsel, K. Iron-organic matter complexes accelerate microbial iron cycling in an iron-rich fen. *Sci. Total Environ.* **2019**, *646*, 972−988.
(11) Luther, G. W.; Kostka, J. E.; Church, T. M.; Sulzberger, B.; Stumm, W. Seasonal iron cycling in the salt-marsh sedimentary environment: the importance of ligand complexes with Fe(II) and Fe(III) in the dissolution of Fe(III) minerals and pyrite, respectively. *Mar. Chem.* **1992**, *40*, 81−103.
(12) Sundman, A.; Karlsson, T.; Laudon, H.; Persson, P. XAS study of iron speciation in soils and waters from a boreal catchment. *Chem. Geol.* **2014**, *364*, 93−102.
(13) Kleber, M.; Bourg, I. C.; Coward, E. K.; Hansel, C. M.; Myneni, S. C. B.; Nunan, N. Dynamic interactions at the mineral−organic matter interface. *Nat. Rev. Earth Environ.* **2021**, *2*, 402−421.
(14) Lalonde, K.; Mucci, A.; Ouellet, A.; Gélinas, Y. Preservation of organic matter in sediments promoted by iron. *Nature* **2012**, *483*, 198−200.
(15) Zhao, Q.; Poulson, S. R.; Obrist, D.; Sumaila, S.; Dynes, J. J.; McBeth, J. M.; Yang, Y. Iron-bound organic carbon in forest soils: quantification and characterization. *Biogeosciences* **2016**, *13*, 4777−4788.
(16) Wagai, R.; Mayer, L. M.; Kitayama, K.; Shirato, Y. Association of organic matter with iron and aluminum across a range of soils determined via selective dissolution techniques coupled with dissolved nitrogen analysis. *Biogeochemistry* **2013**, *112*, 95−109.
(17) Mu, C. C.; Zhang, T. J.; Zhao, Q.; Guo, H.; Zhong, W.; Su, H.; Wu, Q. B. Soil organic carbon stabilization by iron in permafrost regions of the Qinghai-Tibet Plateau. *Geophys. Res. Lett.* **2016**, *43*, 10286−10294.
(18) Coward, E. K.; Thompson, A. T.; Plante, A. F. Iron-mediated mineralogical control of organic matter accumulation in tropical soils. *Geoderma* **2017**, *306*, 206−216.
(19) Rue, E. L.; Bruland, K. W. Complexation of iron(III) by natural organic ligands in the Central North Pacific as determined by a new competitive ligand equilibration/adsorptive cathodic stripping voltammetric method. *Mar. Chem.* **1995**, *50*, 117−138.
(20) Faust, J. C.; Tessin, A.; Fisher, B. J.; Zindorf, M.; Papadaki, S.; Hendry, K. R.; Doyle, K. A.; März, C. Millennial scale persistence of organic carbon bound to iron in Arctic marine sediments. *Nat. Commun.* **2021**, *12*, 275.
(21) Hudson, J. M.; Luther, G. W.; Chin, Y.-P. Influence of Organic Ligands on the Redox Properties of Fe(II) as Determined by Mediated Electrochemical Oxidation. *Environ. Sci. Technol.* **2022**, *56*, 9123−9132.
(22) Strathmann, T. J. *Aquatic Redox Chemistry*; ACS Symposium Series; American Chemical Society, 2011; Vol. *1071*, Chapter 14, pp 283−313.
(23) Peng, C.; Bryce, C.; Sundman, A.; Borch, T.; Kappler, A. Organic Matter Complexation Promotes Fe(II) Oxidation by the Photoautotrophic Fe(II)-Oxidizer Rhodopseudomonas palustris TIE-1. *ACS Earth Space Chem.* **2019**, *3*, 531−536.
(24) Daugherty, E. E.; Gilbert, B.; Nico, P. S.; Borch, T. Complexation and Redox Buffering of Iron(II) by Dissolved Organic Matter. *Environ. Sci. Technol.* **2017**, *51*, 11096−11104.
(25) Chen, C.; Thompson, A. Ferrous Iron Oxidation under Varying pO2 Levels: The Effect of Fe(III)/Al(III) Oxide Minerals and Organic Matter. *Environ. Sci. Technol.* **2018**, *52*, 597−606.
(26) Theis, T. L.; Singer, P. C. Complexation of iron(II) by organic matter and its effect on iron(II) oxygenation. *Environ. Sci. Technol.* **1974**, *8*, 569−573.
(27) Gledhill, M.; Buck, K. The Organic Complexation of Iron in the Marine Environment: A Review. *Front. Microbiol.* **2012**, *3*, 69.
(28) Jones, A. M.; Griffin, P. J.; Waite, T. D. Ferrous iron oxidation by molecular oxygen under acidic conditions: The effect of citrate, EDTA and fulvic acid. *Geochim. Cosmochim. Acta* **2015**, *160*, 117−131.
(29) Pham, A. N.; Waite, T. D. Oxygenation of Fe(II) in the Presence of Citrate in Aqueous Solutions at pH 6.0−8.0 and 25 °C:

Interpretation from an Fe(II)/Citrate Speciation Perspective. *J. Phys. Chem. A* **2008**, *112*, 643−651.
(30) Pullin, M. J.; Cabaniss, S. E. The effects of pH, ionic strength, and iron−fulvic acid interactions on the kinetics of non-photochemical iron transformations. I. Iron(II) oxidation and iron(III) colloid formation. *Geochim. Cosmochim. Acta* **2003**, *67*, 4067−4077.
(31) Liang, L.; McNabb, J. A.; Paulk, J. M.; Gu, B.; McCarthy, J. F. Kinetics of iron(II) oxygenation at low partial pressure of oxygen in the presence of natural organic matter. *Environ. Sci. Technol.* **1993**, *27*, 1864−1870.
(32) Chen, C.; Thompson, A. The influence of native soil organic matter and minerals on ferrous iron oxidation. *Geochim. Cosmochim. Acta* **2021**, *292*, 254−270.
(33) Chen, C.; Hall, S. J.; Coward, E.; Thompson, A. Iron-mediated organic matter decomposition in humid soils can counteract protection. *Nat. Commun.* **2020**, *11*, 2255.
(34) von Lützow, M.; Kögel-Knabner, I.; Ekschmitt, K.; Flessa, H.; Guggenberger, G.; Matzner, E.; Marschner, B. SOM fractionation methods: Relevance to functional pools and to stabilization mechanisms. *Soil Biol. Biochem.* **2007**, *39*, 2183−2207.
(35) Gorham, E. Northern Peatlands: Role in the Carbon Cycle and Probable Responses to Climatic Warming. *Ecol. Appl.* **1991**, *1*, 182−195.
(36) Hartnett, H. E. In *Encyclopedia of Geochemistry: A Comprehensive Reference Source on the Chemistry of the Earth*; White, W. M., Ed.; Springer International Publishing: Cham, 2018; pp 375−378.
(37) Lavallee, J. M.; Soong, J. L.; Cotrufo, M. F. Conceptualizing soil organic matter into particulate and mineral-associated forms to address global change in the 21st century. *Global Change Biol.* **2020**, *26*, 261−273.
(38) Tfaily, M. M.; Cooper, W. T.; Kostka, J. E.; Chanton, P. R.; Schadt, C. W.; Hanson, P. J.; Iversen, C. M.; Chanton, J. P. Organic matter transformation in the peat column at Marcell Experimental Forest: Humification and vertical stratification. *J. Geophys. Res.: Biogeosci.* **2014**, *119*, 661−675.
(39) Karlsson, T.; Persson, P.; Skyllberg, U.; Mörth, C. M.; Giesler, R. Characterization of Iron(III) in Organic Soils Using Extended X-ray Absorption Fine Structure Spectroscopy. *Environ. Sci. Technol.* **2008**, *42*, 5449−5454.
(40) Bhattacharyya, A.; Schmidt, M. P.; Stavitski, E.; Martínez, C. E. Iron speciation in peats: Chemical and spectroscopic evidence for the co-occurrence of ferric and ferrous iron in organic complexes and mineral precipitates. *Org. Geochem.* **2018**, *115*, 124−137.
(41) Patzner, M. S.; Mueller, C. W.; Malusova, M.; Baur, M.; Nikeleit, V.; Scholten, T.; Hoeschen, C.; Byrne, J. M.; Borch, T.; Kappler, A.; Bryce, C. Iron mineral dissolution releases iron and associated organic carbon during permafrost thaw. *Nat. Commun.* **2020**, *11*, 6329.
(42) Chen, C.; Dong, Y.; Thompson, A. Electron Transfer, Atom Exchange, and Transformation of Iron Minerals in Soils: The Influence of Soil Organic Matter. *Environ. Sci. Technol.* **2023**, *57*, 10696−10707.
(43) Blodau, C. Carbon cycling in peatlands: A review of processes and controls. *Environ. Rev.* **2002**, *10*, 111−134.
(44) Hornibrook, E. R. C.; Longstaffe, F. J.; Fyfe, W. S.; Bloom, Y. Carbon-isotope ratios and carbon, nitrogen and sulfur abundances in flora and soil organic matter from a temperate-zone bog and marsh. *Geochem. J.* **2000**, *34*, 237−245.
(45) Moore, T.; Blodau, C.; Turunen, J.; Roulet, N.; Richard, P. J. H. Patterns of nitrogen and sulfur accumulation and retention in ombrotrophic bogs, eastern Canada. *Global Change Biol.* **2005**, *11*, 356−367.
(46) Joshi, P.; Schroth, M. H.; Sander, M. Redox Properties of Peat Particulate Organic Matter: Quantification of Electron Accepting Capacities and Assessment of Electron Transfer Reversibility. *J. Geophys. Res.: Biogeosci.* **2021**, *126*, No. e2021JG006329.
(47) Beer, J.; Lee, K.; Whiticar, M.; Blodau, C. Geochemical controls on anaerobic organic matter decomposition in a northern peatland. *Limnol. Oceanogr.* **2008**, *53*, 1393−1407.
(48) Klüpfel, L.; Piepenbrock, A.; Kappler, A.; Sander, M. Humic substances as fully regenerable electron acceptors in recurrently anoxic environments. *Nat. Geosci.* **2014**, *7*, 195−200.
(49) Stookey, L. L. Ferrozine—a new spectrophotometric reagent for iron. *Anal. Chem.* **1970**, *42*, 779−781.
(50) Ravel, B.; Newville, M. ATHENA, ARTEMIS, HEPHAESTUS: data analysis for X-ray absorption spectroscopy using IFEFFIT. *J. Synchrotron Radiat.* **2005**, *12*, 537−541.
(51) Kelly, S. D.; Hesterberg, D.; Ravel, B. *Methods of Soil Analysis Part 5—Mineralogical Methods*; John Wiley & Sons, Ltd, 2008; Chapter 14, pp 387−463.
(52) Lagarec, K.; Rancourt, D. G. Extended Voigt-based analytic lineshape method for determining N-dimensional correlated hyperfine parameter distributions in Mössbauer spectroscopy. *Nucl. Instrum. Methods Phys. Res., Sect. B* **1997**, *129*, 266−280.
(53) Possinger, A. R.; Bailey, S. W.; Inagaki, T. M.; Kögel-Knabner, I.; Dynes, J. J.; Arthur, Z. A.; Lehmann, J. Organo-mineral interactions and soil carbon mineralizability with variable saturation cycle frequency. *Geoderma* **2020**, *375*, 114483.
(54) Catrouillet, C.; Davranche, M.; Dia, A.; Bouhnik-Le Coz, M.; Marsac, R.; Pourret, O.; Gruau, G. Geochemical modeling of Fe(II) binding to humic and fulvic acids. *Chem. Geol.* **2014**, *372*, 109−118.
(55) Sparks, D. L. In *Environmental Soil Chemistry*, 2nd ed.; Sparks, D. L., Ed.; Academic Press: Burlington, 2003; pp 75−113.
(56) Yamamoto, M.; Nishida, A.; Otsuka, K.; Komai, T.; Fukushima, M. Evaluation of the binding of iron(II) to humic substances derived from a compost sample by a colorimetric method using ferrozine. *Bioresour. Technol.* **2010**, *101*, 4456−4460.
(57) Ritchie, J. D.; Perdue, E. Proton-binding study of standard and reference fulvic acids, humic acids, and natural organic matter. *Geochim. Cosmochim. Acta* **2003**, *67*, 85−96.
(58) Driver, S. J.; Perdue, E. M. *Advances in the Physicochemical Characterization of Dissolved Organic Matter: Impact on Natural and Engineered Systems*; American Chemical Society, 2014; Vol. *1160*, pp 75−86.
(59) Schnitzer, M.; Desjardins, J. G. Carboxyl and Phenolic Hydroxyl Groups in Some Organic Soils and Their Relation to the Degree of Humification. *Can. J. Soil Sci.* **1965**, *45*, 257−264.
(60) Schnitzer, M.; Gupta, U. C. Determination of Acidity in Soil Organic Matter. *Soil Sci. Soc. Am. J.* **1965**, *29*, 274−277.
(61) Armanious, A.; Aeppli, M.; Sander, M. Dissolved Organic Matter Adsorption to Model Surfaces: Adlayer Formation, Properties, and Dynamics at the Nanoscale. *Environ. Sci. Technol.* **2014**, *48*, 9420−9429.
(62) Duval, J. F. L.; Wilkinson, K. J.; van Leeuwen, H. P.; Buffle, J. Humic Substances Are Soft and Permeable: Evidence from Their Electrophoretic Mobilities. *Environ. Sci. Technol.* **2005**, *39*, 6435−6445.
(63) Murad, E.; Cashion, J. *Mössbauer Spectroscopy of Environmental Materials and Their Industrial Utilization*; Kluwer Academic Publishers Group: Dordrecht, The Netherlands, 2004.
(64) Burgess, J. *Ions in Solution: Basic Principles of Chemical Interactions*; Horwood Series in Chemical Science; Elsevier Science, 1999.
(65) Bauer, M.; Heitmann, T.; Macalady, D. L.; Blodau, C. Electron Transfer Capacities and Reaction Kinetics of Peat Dissolved Organic Matter. *Environ. Sci. Technol.* **2007**, *41*, 139−145.
(66) Snoeyink, V. L.; Jenkins, D. *Water Chemistry*; Spe Monographs; Wiley, 1980.
(67) Bhattacharyya, A.; Schmidt, M. P.; Stavitski, E.; Azimzadeh, B.; Martínez, C. E. Ligands representing important functional groups of natural organic matter facilitate Fe redox transformations and resulting binding environments. *Geochim. Cosmochim. Acta* **2019**, *251*, 157−175.


https://doi.org/10.1021/acsearthspacechem.3c00288
*ACS Earth Space Chem.* XXXX, XXX, XXX−XXX

(68) Uchimiya, M.; Stone, A. T. Reversible redox chemistry of quinones: Impact on biogeochemical cycles. *Chemosphere* **2009**, *77*, 451−458.
(69) Aeschbacher, M.; Vergari, D.; Schwarzenbach, R. P.; Sander, M. Electrochemical Analysis of Proton and Electron Transfer Equilibria of the Reducible Moieties in Humic Acids. *Environ. Sci. Technol.* **2011**, *45*, 8385−8394.
(70) Scott, D. T.; McKnight, D. M.; Blunt-Harris, E. L.; Kolesar, S. E.; Lovley, D. R. Quinone Moieties Act as Electron Acceptors in the Reduction of Humic Substances by Humics-Reducing Microorganisms. *Environ. Sci. Technol.* **1998**, *32*, 2984−2989.
(71) Keller, J. K.; Takagi, K. K. Solid-phase organic matter reduction regulates anaerobic decomposition in bog soil. *Ecosphere* **2013**, *4*, 1−12.
(72) Roden, E. E.; Kappler, A.; Bauer, I.; Jiang, J.; Paul, A.; Stoesser, R.; Konishi, H.; Xu, H. Extracellular electron transfer through microbial reduction of solid-phase humic substances. *Nat. Geosci.* **2010**, *3*, 417−421.
(73) Walpen, N.; Getzinger, G. J.; Schroth, M. H.; Sander, M. Electron-Donating Phenolic and Electron-Accepting Quinone Moieties in Peat Dissolved Organic Matter: Quantities and Redox Transformations in the Context of Peat Biogeochemistry. *Environ. Sci. Technol.* **2018**, *52*, 5236−5245.
(74) Clark, W. M. *Oxidation-Reduction Potentials of Organic Systems*; Williams & Wilkins, 1960.
(75) Jiang, C.; Garg, S.; Waite, T. D. Hydroquinone-Mediated Redox Cycling of Iron and Concomitant Oxidation of Hydroquinone in Oxic Waters under Acidic Conditions: Comparison with Iron−Natural Organic Matter Interactions. *Environ. Sci. Technol.* **2015**, *49*, 14076−14084.
(76) Obradović, N.; Joshi, P.; Arn, S.; Aeppli, M.; Schroth, M. H.; Sander, M. Reoxidation of Reduced Peat Organic Matter by Dissolved Oxygen: Combined Laboratory Column-Breakthrough Experiments and In-Field Push-Pull Tests. *J. Geophys. Res.: Biogeosci.* **2023**, *128*, No. e2023JG007640.
(77) Zhou, Z.; Latta, D. E.; Noor, N.; Thompson, A.; Borch, T.; Scherer, M. M. Fe(II)-Catalyzed Transformation of Organic Matter-Ferrihydrite Coprecipitates: A Closer Look Using Fe Isotopes. *Environ. Sci. Technol.* **2018**, *52*, 11142−11150.
(78) ThomasArrigo, L. K.; Kaegi, R.; Kretzschmar, R. Ferrihydrite Growth and Transformation in the Presence of Ferrous Iron and Model Organic Ligands. *Environ. Sci. Technol.* **2019**, *53*, 13636−13647.
(79) Byrne, J. M.; Kappler, A. A revised analysis of ferrihydrite at liquid helium temperature using Mössbauer spectroscopy. *Am. Mineral.* **2022**, *107*, 1643−1651.
(80) Chen, J.; Gu, B.; Royer, R. A.; Burgos, W. D. The roles of natural organic matter in chemical and microbial reduction of ferric iron. *Sci. Total Environ.* **2003**, *307*, 167−178.
(81) Stumm, W.; Morgan, J. J. *Aquatic Chemistry; an Introduction Emphasizing Chemical Equilibria in Natural Waters*; Wiley-Interscience, 1970.
(82) King, D. W.; Lounsbury, H. A.; Millero, F. J. Rates and Mechanism of Fe(II) Oxidation at Nanomolar Total Iron Concentrations. *Environ. Sci. Technol.* **1995**, *29*, 818−824.
(83) Rose, A. L.; Waite, T. D. Kinetic Model for Fe(II) Oxidation in Seawater in the Absence and Presence of Natural Organic Matter. *Environ. Sci. Technol.* **2002**, *36*, 433−444.
(84) Sedlak, D. L.; Hoigné, J. The role of copper and oxalate in the redox cycling of iron in atmospheric waters. *Atmos. Environ., Part A* **1993**, *27*, 2173−2185.
(85) Hansel, C. M.; Benner, S. G.; Neiss, J.; Dohnalkova, A.; Kukkadapu, R. K.; Fendorf, S. Secondary mineralization pathways induced by dissimilatory iron reduction of ferrihydrite under advective flow. *Geochim. Cosmochim. Acta* **2003**, *67*, 2977−2992.
(86) ThomasArrigo, L. K.; Byrne, J. M.; Kappler, A.; Kretzschmar, R. Impact of Organic Matter on Iron(II)-Catalyzed Mineral Transformations in Ferrihydrite−Organic Matter Coprecipitates. *Environ. Sci. Technol.* **2018**, *52*, 12316−12326.


https://doi.org/10.1021/acsearthspacechem.3c00288
*ACS Earth Space Chem.* XXXX, XXX, XXX−XXX